ACTA IMEKO
ISSN: 2221-870X
September 2026, Volume 15, Number 3, 1 – 6

Spiral X-ray computed tomography of long wooden samples: Influence of pitch and geometric calibration on reconstruction quality

Václav Rada[1], Daniel Vavřík[1], Jiří Kunecký[1], Daniel Kytýř[1]

[1] *Czech Academy of Sciences, Institute of Theoretical and Applied Mechanics, Prague, Czechia*

ABSTRACT
X-ray computed tomography (XCT) is widely used for three-dimensional characterization of material microstructure. In wood science, XCT increasingly serves as a tool for quantitative analysis of annual rings, porosity, and other structural features requiring high reconstruction fidelity, and geometrical consistency. Spiral XCT enables scanning of samples exceeding the detector field of view in height by combining continuous sample rotation with synchronized axial translation during acquisition. This work investigates the influence of mechanical alignment, motion synchronization, geometric calibration, and spiral pitch on the reconstruction quality of long wooden specimens. Reconstruction fidelity depends on the agreement between the assumed spiral trajectory and the actual coupled rotational and axial motion during acquisition. Misalignment of the rotation axis with respect to the source–detector geometry, together with inaccuracies in axial translation or magnification calibration, may introduce geometric distortions, blurring, and loss of structural fidelity. The effect of spiral pitch, defined as the axial displacement per full rotation, was experimentally investigated by performing scans with different predefined pitch values. Increasing the spiral pitch reduced axial sampling density and projection overlap, resulting in progressively stronger interpolation artefacts and degradation of reconstruction quality. The study further demonstrates the sensitivity of cone-beam spiral XCT reconstruction to accurate magnification calibration, as even small scaling errors lead to cumulative misregistration along the reconstructed volume. Reliable spiral XCT of long wooden samples therefore requires accurate geometric calibration, stable synchronization of the rotational and axial motions, and an appropriately selected spiral pitch.

Section: RESEARCH PAPER

Keywords: spiral X-ray computed tomography; cone-beam CT; non-destructive testing (NDT); geometric calibration; motion synchronization; spiral pitch

Citation: V. Rada, D. Vavřík, J. Kunecký, D. Kytýř, Spiral X-ray computed tomography of long wooden samples: Influence of pitch and geometric calibration on reconstruction quality, Acta IMEKO, vol. 15 (2026) no. 3, pp. 1–6. DOI: 10.21014/actaimeko.v15i3.2471

Section Editor: Emina Hadzalic, University of Rijeka, Croatia

Received: Juli 27, 2026; **In Final Form:** August 24, 2026; **Published:** September, 2026.

Funding: This research was supported by the Czech Science Foundation (Project No. 25-18144S). D. Kytyr acknowledges the support from OP JAK (Project INODIN CZ.02.01.01/00/23_020/0008487).

Corresponding Author: Daniel Kytýř, e-mail: kytyr@itam.cas.cz

1. INTRODUCTION

Wood is a complex hierarchical biological material whose mechanical behaviour, durability, transport properties, and overall performance are closely linked to its three-dimensional anatomical structure [1]. Consequently, non-destructive imaging techniques capable of resolving the internal morphology of wood have become indispensable tools in modern wood science and engineering [2]. Among these techniques, X-ray computed tomography (XCT) has become well established for the characterization of annual growth rings, vessels, knots, cracks, density variations, and other anatomical features governing the physical and mechanical behaviour of wood [3], [4]. In many applications, quantitative evaluation requires not only high spatial resolution but also geometrically accurate, continuous volumetric imaging over extended specimen lengths, enabling structural features to be analysed without interruptions or stitching artefacts [5].

Conventional laboratory cone-beam XCT systems are limited by the available field of view, which is determined by the detector dimensions and the imaging geometry [6]. Although reducing the geometric magnification increases the accessible imaging volume, it inevitably compromises spatial resolution. This trade-off is particularly limiting for elongated specimens, for which only a limited portion can be reconstructed in a single scan. While sequential scanning combined with volume stitching can partially overcome this limitation, it increases experimental and computational complexity and may reduce geometric consistency [7]. Consequently, acquisition strategies capable of extending the reconstructed volume while preserving high spatial resolution are of considerable practical interest.

Spiral X-ray computed tomography (spiral XCT) extends conventional cone-beam acquisition by combining continuous sample rotation with synchronized axial translation, enabling the reconstruction of specimens exceeding the detector field of view in the axial direction [8]. Originally developed for medical computed tomography, the technique has subsequently been adopted in laboratory cone-beam XCT systems, where several custom-built and application-specific implementations have demonstrated its potential for imaging elongated specimens while preserving high spatial resolution [9]. Despite these advances, laboratory spiral XCT remains considerably less mature than conventional cone-beam XCT, and its practical implementation is often closely coupled to the specific hardware configuration and acquisition software of individual systems [10].

Although the feasibility of laboratory spiral XCT has been demonstrated in several application-specific studies, including the imaging of elongated engineering structures [11], [12], considerably less attention has been paid to the metrological aspects governing reconstruction quality. In particular, the influence of acquisition parameters and geometric calibration on reconstruction fidelity has not been systematically evaluated for laboratory cone-beam XCT systems. Since these factors determine the correspondence between the physical acquisition trajectory and the reconstruction model, their accurate implementation is essential for obtaining geometrically consistent and quantitatively reliable volumetric data [13].

Motivated by the need for high-resolution imaging of elongated wooden specimens, an in-house spiral acquisition workflow was implemented on a laboratory cone-beam XCT system. This study experimentally investigates the influence of spiral pitch, motion synchronization, geometric calibration, and magnification calibration on reconstruction fidelity, and assesses their effect on the geometric consistency of reconstructed volumes. The presented methodology and findings provide practical guidance for the implementation and optimization of laboratory spiral XCT, and are generally applicable to the imaging of elongated specimens beyond wood science.

2. MEASUREMENT SETUP

The experiments were performed using an in-house developed laboratory cone-beam X-ray computed tomography (XCT) system configured for both conventional and spiral scanning. The imaging hardware and system architecture have been described previously [14], while the acquisition control framework is presented in detail in [15]. The system consists of a microfocus X-ray source (Hamamatsu L10321), a flat-panel X-ray detector (Dexela 1512 NDT), and a motorized sample manipulation system enabling synchronized rotational and vertical motion, as shown in Figure 1. The detector has an active imaging area of 1944×1536 pixels with a nominal pixel size of 74.8 µm, providing high-resolution projection images suitable for microstructural characterization.

The specimen is mounted on a high-precision rotary stage positioned between the X-ray source and detector. During conventional CT acquisition, the sample rotates through 360° while remaining at a fixed vertical position. For spiral XCT, the rotary stage is synchronized with the vertical translation of the X-ray source and detector, resulting in a helical acquisition trajectory. The spiral pitch is defined as the vertical displacement during one complete revolution.

The imaging geometry is defined by the source-to-object distance (SOD) and the source-to-detector distance (SDD), which determine the geometric magnification. Both the X-ray source and detector are mounted on precision translation stages, allowing independent adjustment of SOD and SDD. In addition, the detector assembly permits fine adjustment of detector tilt, while the source and detector positions can be adjusted in both horizontal and vertical directions to establish the desired imaging geometry.

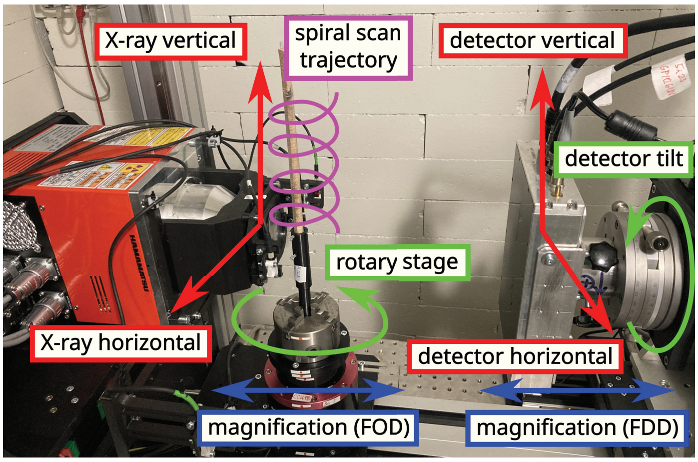

Figure 1. Schematic image of the CT apparatus and the controlled axes.

Accurate geometric calibration is essential for spiral reconstruction. The alignment of the X-ray source, detector, and rotary axis, together with the synchronization between rotational and vertical motion, defines the agreement between the actual acquisition trajectory and the reconstruction model. Deviations in detector orientation, magnification, or vertical translation introduce geometric inconsistencies that may result in reconstruction artifacts and reduced image quality.

2.1. Sample

English oak (*Quercus robur* L.) was selected as the model material because its well-defined annual-ring structure provides a suitable specimen for assessing the geometrical consistency and reconstruction quality of spiral XCT. The investigated specimens were collected from trees growing under near-optimal site conditions in the Drahanská vrchovina region of South Moravia, Czech Republic. The sampled trees were approximately 100 years old.

To preserve a continuous sequence of approximately 100 annual rings, cylindrical cores approximately 28 cm long were extracted using a hollow drill. Such specimen length exceeded the axial field of view of the XCT system and therefore required spiral acquisition. The reconstructed datasets are intended for subsequent analysis of wood structure and density distribution. For density calibration, rubber reference blocks with known density were attached to the top of each specimen (Figure 5).

The specimen diameter of approximately 10 mm required additional mechanical stabilization during XCT acquisition. Each specimen was enclosed in a heat-shrink tube to increase its stiffness and minimize deformation or unwanted motion during scanning. This mounting approach improved the stability of the acquisition and contributed to consistent reconstruction quality (Figure 6).

2.2. XCT imaging

The XCT acquisition was performed using a high-resolution cone-beam configuration operating in spiral (helical) scan mode. A total of 1912 projections were acquired over a full 360° rotation, with continuous rotation and synchronized vertical motion of the X-ray source and detector. Each projection was recorded with an exposure time of 115 ms, and no averaging was applied. Projection data were recorded as 14-bit unsigned integers without detector binning, resulting in an isotropic reconstructed voxel size of 11.23 µm × 11.23 µm × 11.23 µm.

Beam conditioning was achieved using an aluminium filter of 0.3 mm thickness, which reduces low-energy photons and mitigates beam-hardening artefacts. The X-ray source was operated at 70 kV and 100 µA, corresponding to a tube power of 7 W. The focal spot size was approximately 9.7 µm, providing a suitable balance between spatial resolution and photon flux for high-resolution microstructural imaging.

The imaging geometry was defined by a SOD of 41.96 mm and a SDD of 280.26 mm, resulting in a geometric magnification of approximately 6.69. These distances were set using precision translation stages, enabling stable and reproducible magnification conditions throughout the scan. Fine adjustments of detector position and tilt were performed, while the source and detector positions were aligned in both horizontal and vertical directions to establish the desired imaging geometry.

In spiral XCT mode, the specimen rotation is synchronised with vertical translation of the X-ray source and detector, resulting in a helical imaging trajectory. The spiral pitch is defined by the vertical displacement per full rotation and determines the axial sampling density along the scanned volume. Compared with conventional circular cone-beam CT, this acquisition strategy enables extended field-of-view coverage in the vertical direction without discontinuities between individual scan segments.

During the acquisition, 28 spiral rotations were performed with a spiral pitch of 10 mm per rotation, resulting in a total scan length of approximately 280 mm. This acquisition strategy provided continuous volumetric coverage of the entire specimen while maintaining consistent projection overlap between successive rotations. In total, approximately 53,500 projections were acquired, corresponding to approximately 300 GB of raw projection data. The tomographic data were reconstructed using the proprietary Helix reconstruction algorithm implemented in VGStudio MAX 2025.1 (Volume Graphics GmbH, Germany). The reconstruction was performed on a workstation equipped with an Intel Xeon W-2265 CPU (3.50 GHz), 512 GB of RAM, and an NVIDIA Quadro RTX 4000 GPU with 8 GB of memory. The complete dataset was reconstructed in approximately 7 h.

Accurate geometric calibration is critical for spiral reconstruction. The system alignment, including source, detector, and rotational axis positioning, together with precise synchronization between rotational and vertical motion, ensures consistency between the physical helical trajectory and the reconstruction model. Any deviations in stage synchronization, detector tilt, or magnification calibration can introduce geometric inconsistencies, leading to reconstruction artefacts and degradation of reconstruction quality.

2.3. Geometrical alignment

Accurate geometric alignment is essential for high-quality XCT reconstruction, since even small deviations in the relative positions of the X-ray source, rotation axis, and detector introduce systematic errors into the projection geometry. These errors propagate directly into the reconstructed volume, causing geometric distortions, image blurring, and reconstruction artefacts that compromise both dimensional accuracy and quantitative evaluation.

A precision geometric calibration procedure was performed using X-ray projections of a steel bar with known diameter acquired at two different magnifications, as illustrated in Figure 2. The known object size served as a dimensional reference to refine the system geometry and to accurately align the focal spot, rotation axis, and detector center. For each magnification setting, two complementary fitting strategies were applied to the projected

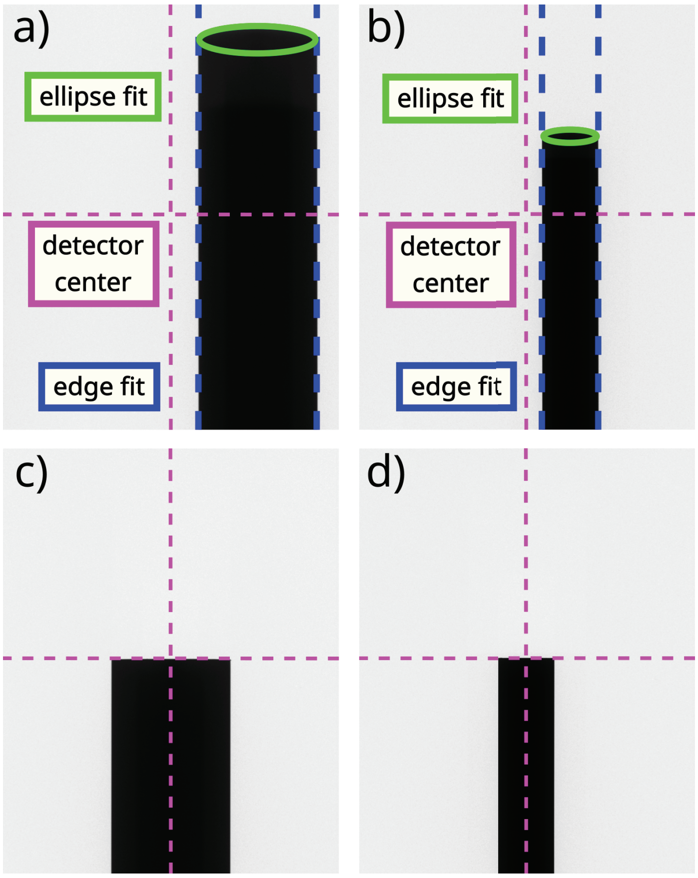

Figure 2. Alignment of the focal spot, rotational axis and the detector using steel bar: a) Image of the misaligned geometry at higher magnification, b) Image of the misaligned geometry at lower magnification, c) Image of the aligned geometry at higher magnification, d) Image of the aligned geometry at lower magnification.

bar silhouette. An edge-fitting approach was first used in the horizontal direction to robustly detect the lateral boundaries of the bar, providing sub-pixel estimates of the left and right edges and enabling accurate horizontal centering relative to the detector coordinate system. In parallel, an ellipse-fitting model was applied to the projected cross-section to account for geometric distortion due to magnification and beam divergence, allowing precise estimation of the vertical alignment and the apparent deformation of the cylindrical projection. The fitted ellipse center and axes were then used to correct vertical misalignment between the system components. Combining the edge-derived lateral position with the ellipse-derived vertical center enabled a full 2D registration of the steel bar projection in detector space. Based on the calibrated geometry at both magnification settings, the SOD and SDD were subsequently computed, ensuring consistency of the reconstructed system geometry across both imaging configurations. This dual-fitting approach provides a robust framework for high-accuracy geometric calibration in X-ray imaging systems, minimizing alignment errors in both horizontal and vertical directions.

In spiral (helical) tomography, accurate knowledge of the system magnification is particularly important because of the continuous vertical overlap between successive projections acquired along the spiral trajectory. Unlike conventional circular CT, where each projection corresponds to a fixed axial position, spiral reconstruction relies on a precise correspondence between the acquisition geometry and the vertical position of every projection. Consequently, even small errors in geometric magnification accumulate along the spiral trajectory and result in increasing registration errors in the reconstructed volume. For a detector with approximately 2000 pixels in the vertical direction, a relative mag-

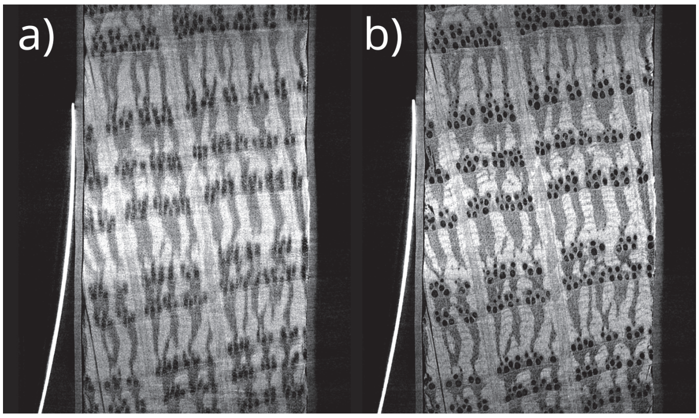

Figure 3. Influence of magnification error on reconstruction quality: a) reconstructed slice with a relative magnification error of 0.1 %, b) reconstructed slice with precisely estimated magnification, All other reconstruction parameters were kept unchanged; the corresponding acquisition and reconstruction conditions are described in Section 2.2..

nification error of only 0.1 % corresponds to a vertical misregistration of approximately two pixels in the reconstructed volume. Such an error is sufficient to introduce noticeable blurring and loss of fine structural detail due to inconsistent voxel alignment between adjacent projections, as demonstrated in Figure 3. In physical terms, for a SOD of 41.96 mm, a 0.1 % magnification error corresponds to an absolute deviation of approximately 40 µm. Although this deviation appears negligible in absolute terms, it significantly degrades the coherence of the back-projected rays in high-resolution spiral XCT, leading to visible deterioration of reconstruction quality. Consequently, accurate magnification calibration is essential for maintaining spatial consistency and reconstruction fidelity in spiral XCT.

2.4. Spiral pitch

The pitch of 10 mm used for the main acquisition corresponds to approximately 46 % of the vertical field of view, providing more than 50 % overlap between successive rotations. Increased overlap generally improves reconstruction quality and axial resolution, although at the expense of increased acquisition time and data volume [16]. To evaluate the influence of spiral pitch on reconstruction quality, four additional pitch values of 8 mm, 12 mm, 16 mm, and 20 mm per full rotation were investigated, corresponding to approximately 37 %, 55 %, 73 %, and 92 % of the vertical field of view, respectively. The selected range therefore covers conditions with both substantial and progressively reduced overlap between successive rotations. All other acquisition and reconstruction parameters were kept unchanged to isolate the influence of spiral pitch. The resulting reconstructions, shown in Figure 4, were compared in terms of reconstruction quality and the occurrence of interpolation artefacts.

3. RESULTS

The developed spiral XCT acquisition procedure enabled successful reconstruction of the entire wooden specimen with a total scanned length of approximately 280 mm. The reconstructed volume was obtained with an isotropic voxel size of approximately 10 µm (11.23 µm in the present acquisition), providing sufficient spatial resolution to resolve the anatomical features investigated in this study. Figure 5 presents the longitudinal reconstructed slice covering the complete specimen. Despite the considerable sample length, the reconstruction exhibits continuous anatomical features without visible discontinuities between successive spiral revolutions, indicating successful synchronization of the rotational and vertical motions throughout the acquisition.

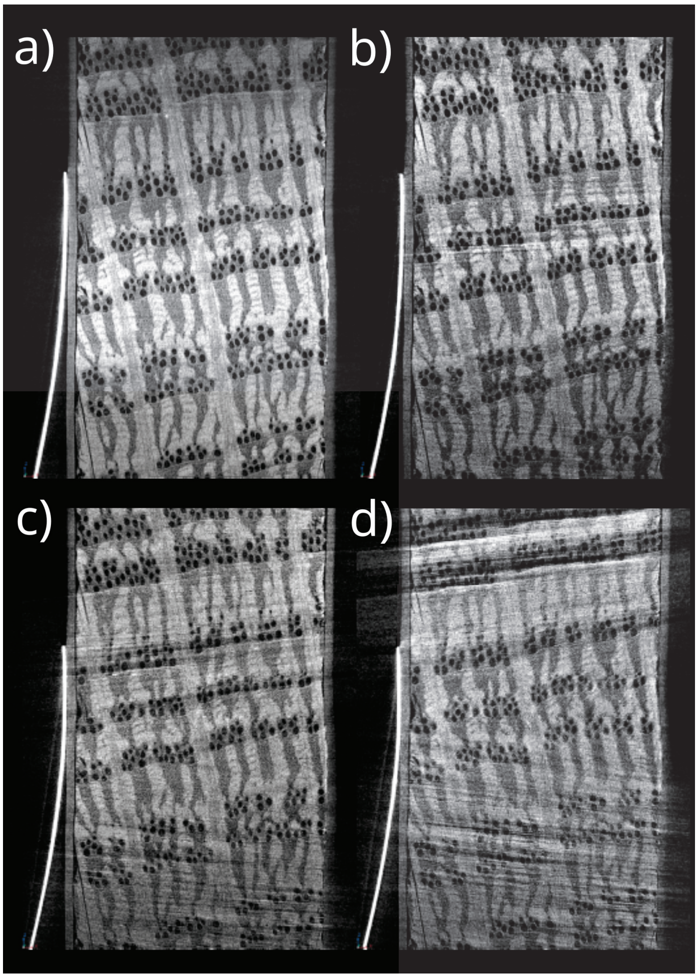

Figure 4. Influence of spiral pitch on reconstruction quality: a) 8 mm, b) 12 mm, c) 16 mm, and d) 20 mm per full rotation. All other acquisition and reconstruction parameters were kept unchanged; the corresponding experimental conditions are described in Section 2.2..

The reconstructed volume shows a well-preserved internal wood structure along the entire specimen. Annual growth rings remain continuous over the full scan length, indicating that the spiral trajectory and reconstruction geometry maintained sufficient geometric consistency during the acquisition. No noticeable stitching artefacts or intensity discontinuities are observed at the transitions between adjacent spiral turns, confirming the geometric consistency of the spiral acquisition and reconstruction.

Figure 6 illustrates a magnified region of the reconstructed specimen. The anatomical features of the hardwood are clearly resolved, including vessels, fibres, rays, and annual growth ring boundaries. Large vessels appear as low-attenuation circular structures distributed throughout the xylem, while differences between earlywood and latewood are visible as periodic variations in X-ray attenuation. The bark can be clearly distinguished from the underlying wood tissue, and the transition between anatomical regions is sharply defined.

The reconstructed images exhibit high spatial resolution with minimal motion-induced blurring, indicating successful synchronization between specimen rotation and the vertical translation of the X-ray source and detector. Fine anatomical features are consistently resolved throughout the reconstructed volume, indicating that the selected acquisition parameters provided adequate sampling density for accurate spiral reconstruction.

The influence of geometric calibration proved to be critical for reconstruction quality. Even small deviations in the estimated mag-

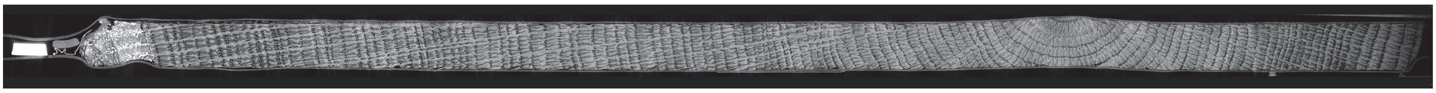

Figure 5. Reconstructed slice of the whole wooden sample, approximately 28 cm of height. Top on the left side, bottom on the right side. At the top of the sample the reference density rubber blocks are placed.

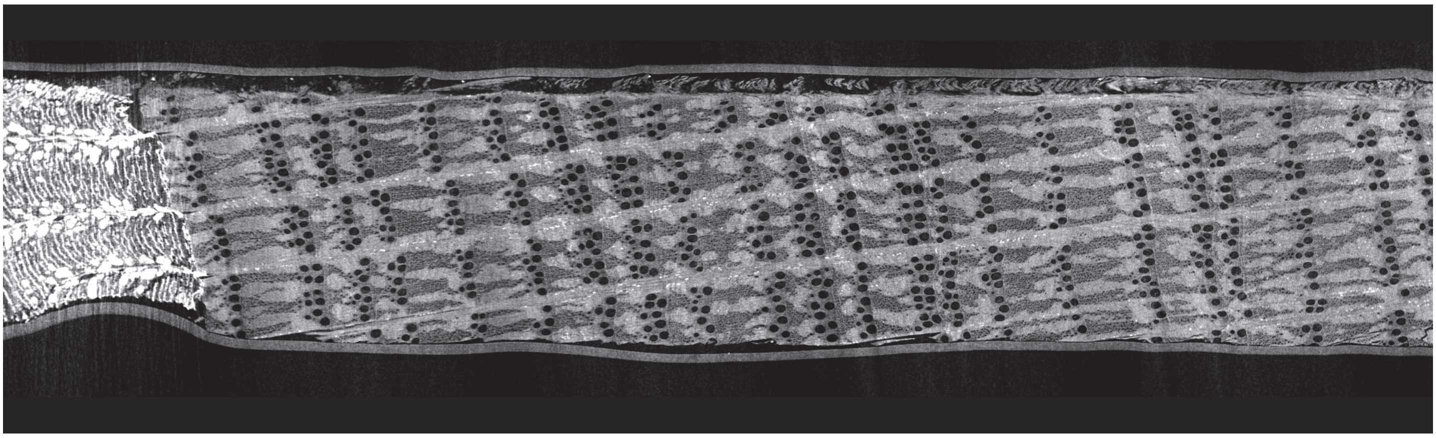

Figure 6. Detailed reconstructed slice of the scanned wooden specimen. The structurally distinct region on the left side of the image corresponds to the outer bark of the specimen. The wood anatomy is clearly resolved, with vessels (pores) appearing as low-attenuation regions distributed throughout the wood structure. Variations in X-ray attenuation reflect local density differences between annual growth layers and anatomical features. The heat-shrink tube surrounding the specimen is also visible.

nification resulted in noticeable degradation of image sharpness and local misregistration of anatomical structures. As demonstrated in Figure 3, a relative magnification error of only 0.1 % introduced visible blurring due to cumulative vertical misalignment of projections during spiral reconstruction. Accurate calibration of the source-to-object and source-to-detector distances therefore represents one of the key requirements for obtaining geometrically consistent reconstructions.

Similarly, the spiral pitch significantly affected reconstruction fidelity, as demonstrated in Figure 4. Lower pitch values produced higher projection redundancy and smoother reconstruction of anatomical structures, whereas increasing the pitch progressively reduced axial sampling density. At pitches above approximately 12 mm per revolution, which corresponds to more than 50 % of the vertical field of view, interpolation artefacts became increasingly apparent, leading to reduced edge sharpness, slight intensity modulation, and local discontinuities of repetitive anatomical features. The largest investigated pitch (20 mm) generated the strongest artefacts, confirming that excessive pitch decreases reconstruction robustness due to insufficient overlap between consecutive helical trajectories.

Overall, the presented results demonstrate that high-resolution spiral XCT enables continuous volumetric imaging of elongated wooden specimens when accurate geometric calibration, precise stage synchronization, and an appropriate spiral pitch are employed. Under these conditions, the reconstructed volumes provide sufficient image quality for quantitative analysis of wood anatomy, density distribution, growth-ring morphology, and other microstructural characteristics.

4. CONCLUSIONS

This study investigated the influence of acquisition geometry and reconstruction parameters on high-resolution spiral X-ray computed tomography (XCT) of elongated wooden specimens.

The results demonstrate that spiral XCT enables continuous volumetric imaging of specimens substantially exceeding the detector field of view while preserving high spatial resolution and anatomical continuity. The implemented helical acquisition workflow successfully reconstructed a specimen approximately 280 mm in length without visible discontinuities, demonstrating the suitability of spiral XCT for imaging elongated wooden samples.

Geometric calibration was identified as the most critical factor affecting reconstruction quality. Accurate calibration of the imaging geometry, including magnification, source and detector positions, and rotation-axis alignment, proved essential for maintaining geometric consistency throughout the reconstructed volume. Even small magnification errors resulted in cumulative projection misregistration and visible degradation of reconstruction quality.

The spiral pitch also had a significant influence on reconstruction fidelity. Lower pitch values increased projection overlap and reconstruction robustness, whereas larger pitches reduced axial sampling density and promoted interpolation artefacts. The presented results highlight the sensitivity of spiral XCT to geometric calibration accuracy and acquisition parameter selection, providing practical guidance for the implementation and optimization of laboratory spiral XCT systems.

The reconstructed datasets clearly resolved key anatomical features of wood, including annual growth rings, vessels, fibres, and bark, demonstrating the suitability of spiral XCT for quantitative characterization of elongated wooden specimens. Future work will focus on objective image-quality assessment using quantitative metrics such as signal-to-noise ratio, measures of spatial resolution and structural continuity, and, where an appropriate reference dataset is available, the structural similarity index. Wood-specific quantitative descriptors of annual-ring and vessel morphology will also be considered for assessing the preservation of anatomical features. These quantitative approaches will support further optimization of acquisition parameters for different wood species and automated analysis of large reconstructed datasets.

AUTHORS' CONTRIBUTION

Václav Rada: Methodology, Investigation, Software, Visualization, Writing – original draft.

Daniel Vavřík: Methodology, Investigation, Visualization, Writing – review & editing.

Jiří Kunecký: Conceptualization, Methodology, Funding acquisition, Writing – original draft.

Daniel Kytýř: Conceptualization, Methodology, Investigation, Writing – review & editing.

DATA AVAILABILITY STATEMENT

Representative experimental data supporting this study are publicly available in the Zenodo repository (DOI: 10.5281/zenodo.21356424) in the form of a reconstructed three-dimensional spiral XCT volume.

ACKNOWLEDGEMENT

This research was supported by the Czech Science Foundation (Project No. 25-18144S). D. Kytyr acknowledges the support from OP JAK (Project INODIN CZ.02.01.01/00/23_020/0008487).

REFERENCES

[1] P. Hass, F. K. Wittel, S. A. McDonald, F. Marone, M. Stampanoni, H. J. Herrmann, P. Niemz, Pore space analysis of beech wood: The vessel network, Holzforschung, vol. 64, 2010, no. 5. DOI: 10.1515/hf.2010.103

[2] B. Bajić, J. A. Huber, B. Neyses, L. Olofsson, O. Öktem, Sparse view tomographic reconstruction of elongated objects using learned primal-dual networks, Engineering Applications of Artificial Intelligence, vol. 162, 2025, p. 112295. DOI: 10.1016/j.engappai.2025.112295

[3] R. J. Ross, Wood handbook: wood as an engineering material, USDA Forest Service, 2010. DOI: 10.2737/fpl-gtr-190

[4] J. Kunecký, M. Hataj, J. Jochman, J. Pošta, M. Kloiber, V. Sebera, Strain-based approach to characterize mode I crack propagation in Norway Spruce directly from optical data, 2024. DOI: 10.21203/rs.3.rs-3962450/v1

[5] A. Popa, J. Jevšenak, M. Dyderski, R. Puchałka, A. Buras, I. Popa, M. Wilmking, A. Kalisty, (with another 46 authors), Spatiotemporal variability of dendroecological indicators in Pedunculate Oak (*Quercus robur* l.) tree-rings across europe in relation to species distribution models, Global Change Biology, vol. 31, 2025, no. 11. DOI: 10.1111/gcb.70567

[6] R. Gupta, M. Grasruck, C. Suess, S. H. Bartling, B. Schmidt, K. Stierstorfer, S. Popescu, T. Brady, T. Flohr, Ultra-high resolution flat-panel volume CT: fundamental principles, design architecture, and system characterization, European Radiology, vol. 16, 2006, no. 6, p. 1191–1205. DOI: 10.1007/s00330-006-0156-y

[7] B. Beeksma, D. Truant, L. Holloway, S. Arumugam, An assessment of image distortion and CT number accuracy within a wide-bore CT extended field of view, Australasian Physical & Engineering Sciences in Medicine, vol. 38, 2015, no. 2, p. 255–261. DOI: 10.1007/s13246-015-0353-6

[8] J. A. Brink, J. P. Heiken, G. Wang, K. W. McEnery, F. J. Schlueter, M. W. Vannier, Helical CT: principles and technical considerations. RadioGraphics, vol. 14, 1994, no. 4, p. 887–893. DOI: 10.1148/radiographics.14.4.7938775

[9] R. Lindtner, L. Kampik, D. Putzer, M. Klosterhuber, A. K. Pallua, W. Streif, M. Schirmer, G. Degenhart, R. Arora, J. D. Pallua, Advancements in high-resolution computed tomography: Revolutionising bone health micro-research, Bioengineering, vol. 12, 2025, no. 11, p. 1189. DOI: 10.3390/bioengineering12111189

[10] P. A. López-Pérez, O. J. Santos-Sánchez, L. Rodríguez-Guerrero, P. Ordaz, Advanced Control Methods for Industrial Processes: Modeling, Design and Simulation of Emerging Systems in Real Time, Wiley, 2025, ISBN: 9783527844197. DOI: 10.1002/9783527844197

[11] D. Kytyr, P. Koudelka, J. Šleichrt, J. Kylar, R. Hrazdirova, J. Lahodny, X-ray computed tomography for non-destructive evaluation of steel wire ropes: Comparison of laboratory XCT configurations for image quality and damage visualization, Acta IMEKO, vol. 15, 2026, no. 3, pp. 1–7. DOI: 10.21014/actaimeko.v15i3.2456

[12] M. Li, Z. Fang, W. Cong, C. Niu, W. Wu, J. Uher, J. Bennett, J. T. Rubinstein, G. Wang, Clinical micro-CT empowered by interior tomography, robotic scanning, and deep learning, IEEE Access, vol. 8, 2020, p. 229018–229032. DOI: 10.1109/access.2020.3046187

[13] M. Grewar, G. Myers, A. Kingston, Practical global backprojection-convolution in transmission cone-beam computed tomography, arXiv: [physics.med-ph], 2024. DOI: 10.48550/arXiv.2412.04669

[14] D. Kytýř, L. Zárybnická, V. Rada, P. Zlámal, P. Koudelka, J. Machotová, J. Šleichrt, R. Ševčík, Full-field deformation characteristics of preserved sandstone via automated 4D X-ray CT procedure, Measurement, vol. 258, 2026, p. 119495. DOI: 10.1016/j.measurement.2025.119495

[15] D. Vavřík, T. Fíla, P. Koudelka, D. Kytýř, M. Macháček, V. Rada, J. Valach, P. Zlámal, Phase-locked X-ray computed tomography for modal analysis of periodically oscillating structures, Measurement, vol. 258, 2026, p. 119395. DOI: 10.1016/j.measurement.2025.119395

[16] J. H. Shin, H. K. Lee, C. G. Choi, D. C. Suh, T.-H. Lim, W. Kang, The quality of reconstructed 3d images in multidetector-row helical CT: Experimental study involving scan parameters, Korean Journal of Radiology, vol. 3, 2002, no. 1, p. 49. DOI: 10.3348/kjr.2002.3.1.49